Aerodynamic Modeling and Design Procedures for Unmanned Aerial Vehicle Propeller

Conference Paper · January 2020

DOI: 10.2514/6.2020-0018

Mohamed Yehia Zakaria
Military Technical College

Mostafa Yassin
Military Technical College

Aerodynamic Modeling and Design Procedures for Unmanned Aerial Vehicle Propeller

Mohamed Y. Zakaria *, Omar. E. Abdelhamid†,Mahmoud.M.abdelghafaar‡, Mostafa.M.yassien§
Military Technical College, Aircraft Mechanics Engineering Department, 11766

In this effort, a sequential design procedures based on selected design parameters are used to design a propeller used for unmanned Ariel vehicles applications. Given the engine power in hand as well as the total aircraft drag, a complete aerodynamic design procedures are conducted on a broad range of propeller rpm, chord distribution and twist angle in an iterative process. A complete graphical user interface is obtained and a 3-Dimensional drawing for the proposed designed propeller is implemented allowing a user friendly design tool for such scale.

I. Introduction

The Wright Brothers' propellers [1] were about 80% efficient, compared to about 90% efficiency of nowadats propellers. The design procedures of aircraft propellers have been of interest for many years, since a hundred years ago, the advantage of propeller design and production increased by 10% only. As for particular aircraft design, there are many factors that affect such propeller design, including engine power, operating RPM for the propeller, diameter limitations, aircraft performance requirements (high speed cruise, takeoff, loiter, etc.), noise requirements. As power increases, additional blades are generally required to efficiently utilize the increased power.

The conditions under which a design would have minimum energy loss were stated by A. Betz as early as 1919[2] ; however, no organized procedure for producing such a design is evident in Glauert's work[3]. Those equations which are given by Betz make extensive use of small-angle approximations and relations applicable only to light loading conditions. Theodorsen [4] showed that the Betz condition for minimum energy loss can be applied to heavy loading as well. In 1979, E. Larrabee [5] resurrected the design equations and presented a straightforward procedure for optimum design. However, there are still some challenges : first, small angle approximations are used ; second, the solution for the displacement velocity is accurate only by ignoring small values (light loading), although an approximate correction is suggested for moderate loading ; and last is the missing viscous term in the expressions for the induced velocities. These viscous terms may be included in the design equations to be consistent with the classical propeller analysis in order to enhance the design procedures.

Improvements have been made in the equations and computational procedures for design of propellers and rotors of

∗. Assistant Professor, acting as Department Head, AIAA APATC Member
†. Professor, AIAA Member
‡. Research Assistant
§. Research Assistant

maximum efficiency. An iterative scheme is introduced for accurate calculation of the vortex displacement velocity and the flow angle distribution. Momentum losses due to radial flow can be estimated by either the Prandtl or Goldstein momentum loss function [6]. The methods presented here bring into exact agreement the procedure for design and analysis. Furthermore, the exactness of this agreement makes it possible for an empirical verification of the Betz condition that a constant-displacement velocity across the wake provides a design of maximum propeller efficiency. The design procedures for such helicopter and micro rotors based on blade element theory as well as unsteady strip theory were introduced by Dayhoum et al. [7], Zakaria et al. [8, 9]. Currently most small unmanned aerial vehicles (UAVs) use inexpensive and readily available off the shelf fixed pitch propellers originally designed for radio controlled (RC) plate forms. Selecting the best off the shelf propeller for a UAV or particular mission can become expensive and consume a time and error process due to the complexities of maximizing the efficiency of an electric propulsion system and meeting the performance requirements of the aircraft. In this work a series of modelling steps followed by an iterative process were proposed for designing a low cost propeller for SUAVs applications. The proposed procedures were followed by a series of forces and bending moments act on a rotating propeller due to centrifugal forces and thrust.

II. PROPELLER AERODYNAMICS

In this section the aerodynamics theory and the geometric data will be presented so that one can use such methods for designing and analyzing any type of propellers. The theory and data presented are limited to those needed for the practical design and the evaluation of the performance of the propellers operating over the speed, power, altitude and angle range of a conventional and V/STOL airplanes. In the development of the design and performance evaluation procedures, empirical corrections have been avoided where possible. The empirical corrections and data are only applied where the theory is not available; for instance, at negative thrust and other off-design operating conditions. It is considered important to stay close to the theory wherever possible to provide information for improving the design and correcting any deficiencies.

The basic function of a propeller is to convert shaft torque to shaft thrust with an efficient method. If the propeller is operating at a given free-stream velocity V and is producing a thrust T, the efficiency becomes :

$$\eta = \frac{T * V}{P} \tag{1}$$

The efficiency of a given propeller at any condition depends on the losses due to friction and those losses due to the acceleration of the fluid.

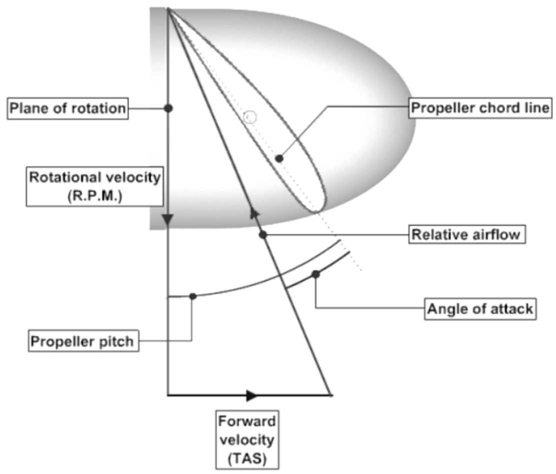

Figure 1 Basic blade section angles

A. Basic propeller dimension

As the purpose of propeller is to give the required thrust with minimum consumed power (the max efficiency), such propellers have aerodynamic profile which should be set to an optimum angle of attack(α_{opt}), consequently corresponds to minimum drag to lift ratio that was determined according to the airfoil and designation and operating Reynold's number. Then the blade needs to be twisted to keep this optimum condition along the blade length. Figure 1 shows the basic section angles of a typical propeller. The aerodynamic design of an aircraft propeller requires a proper choice of design conditions among which the engine characteristics (power, revolutions) as well as the design flight speed. Especially fixed propellers are considerably affected by the design point because their best operation corresponds to a single flight speed only[10] as shown in the following figures (2,3,and 4) :

B. Blade Element momentum Theory (BEM)

The momentum-blade element theory is a relatively simple means to approximate the induced angle of attack (α_i) by combining two different methods (momentum theory and blade element theory).The classical BEMT approach each blade is discretized in a certain number of blade sections along the radius [11]. This approach allows the prediction of propeller performance more accurately by examining the aerodynamics of the blade section. This theory does not particularly account for the flow rotation and tip loss factor, unless it has been imposed. Approximation of the induced effects gives only a rough estimate for the analysis. In general, if the propeller with radius (r) screws itself through the air without slipping, then the distance it would travel in one revolution is the pitch[12] :

$$P = 2\pi r tan\left(\beta\right) \tag{2}$$

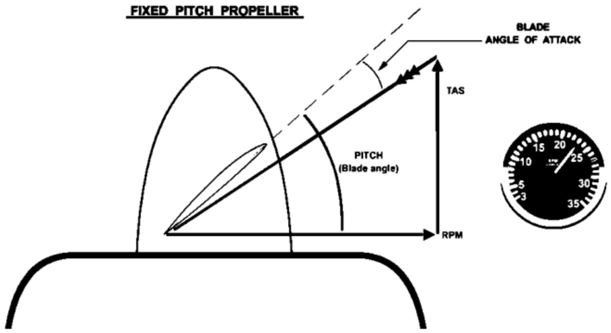

Figure 2 Optimum angle of attack for an operating speed

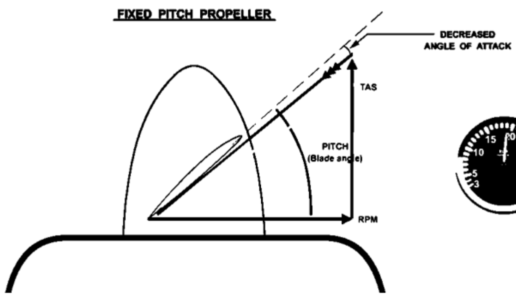

Figure 3 Effect of decreasing operating rmp

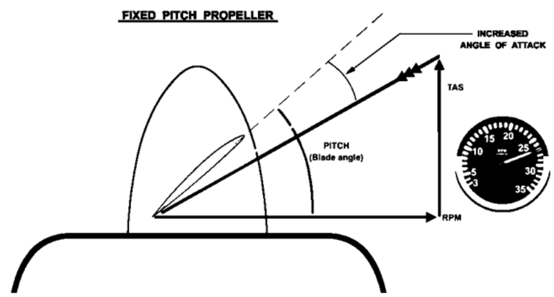

Figure 4 Effect of increasing operating rmp

Assuming the pitch is constant throughout the blade radius, where the pitch angle β is the angle between the plane of rotation and the section chord line. However, for the following analysis, it is more convenient to define it relative to the zero-lift line instead of the chord line. Figure 5 Shows the front view of a rotating propeller with two blades and an angular velocity ω (rad/s) with incoming free stream velocity U. The notation on this figure is similar to that of McCormick [13]. Note that the induced velocity w, shown is much smaller in scale than indicated here.

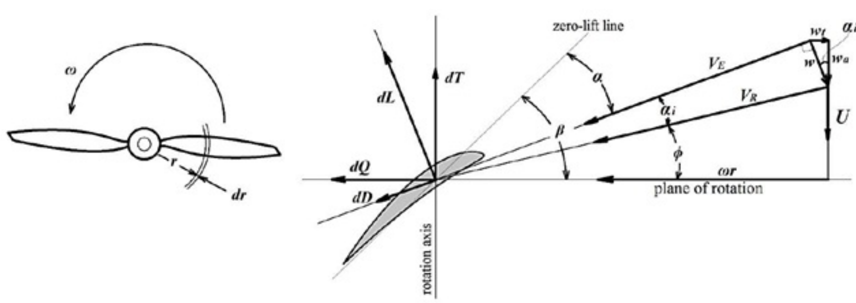

Figure 5 Element forces as described by blade element momentum theory & velocity triangles

The thrust per unit radius , T' acting on the annulus can now be expressed as :

$$T' = \frac{dT}{dr} = 2\pi r \rho V \left(1 + a\right) \left(2VaF\right) \tag{3}$$

By similar arguments, the torque per unit radius Q' is given by :

$$\frac{Q'}{r} = 2\pi r\rho V\left(1+a\right)\left(2r\omega a'F\right) \tag{4}$$

V acts on the blade element with α, and acts on the disc at ϕ. F goes from about (1) at the hub (where the radial flow is typically negligible) to (0) at the tip, and is not unlike the span wise loading of a wing. The functional form of this factor was first estimated by Prandtl [14] and a more accurate, though more complex form was determined by Goldstein [5] . The circulation equations for thrust T ' , and torque Q', per unit radius can be written based on figure 6 as shown :

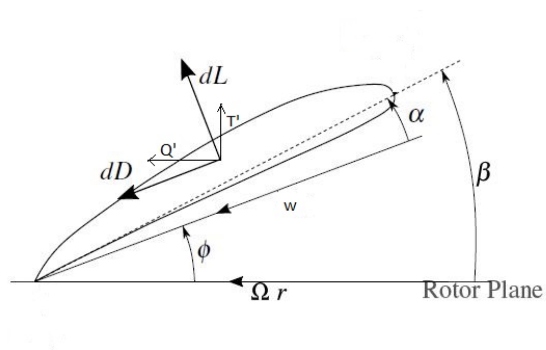

Figure 6 Geometry of the flow at a blade section

$$T' = L'cos\phi - D'sin\phi = L'cos\phi\left(1-\epsilon tan\phi\right) \tag{5}$$

$$Q'r = L'sin\phi + D'cos\phi = L'sin\phi\left(1+\epsilon/tan\phi\right) \tag{6}$$

In order to include Prandtl Tip and Hub Losses Corrections [15], where the original blade element momentum theory does not take into account the influence of vortices shed from the blade tips into the slipstream on the induced velocity field. However, since the blade creates a pressure difference in the flow, at the tip, that flow tends to move from the lower blade surface to the upper blade surface, reducing the resultant force in the neighborhood of the tip. Prandtl, as described in Glauert (1935) [3], derived a correction factor that compensates for the amount of work that can actually be performed by the element according to its proximity to the blade's tip (it is widespread the use of this correction for the blade root too). The factor is calculated as :

$$F = \frac{2}{\pi}\arccos\left(e^{-f}\right) \tag{7}$$

where :

$$f_{tip} = \frac{B}{2}\left(1-\xi\right)/sin\phi_t \tag{8}$$

Similarly, to the f_{tip} presented in Eq. (27) , the f_{hub} can be calculated by :

$$f_{hub} = \frac{B}{2}\left(\xi - 1\right) / sin\phi_t \tag{9}$$

If the element is affected by both tip losses and hub losses, the total factor is obtained by multiplying those factors, but it must be known that the most affecting factor isf_{tip} so we can neglect hub losses factorf_{hub}.

At each radial position along the blade, infinitesimal vortices are shed and move aft as a helicoidal vortex sheet. Since these vortices follow the direction of local flow, the helix angle of the spiral surface is ϕ. The Betz condition for minimum energy loss, neglecting contraction of the wake, requires the vortex sheet to be a regular screw surface ; i.e., (r tan ϕ) must be a constant independent of radius. At the blade station,r, the total lift per unit radius is given by :

$$L' = dL/dr = B\pi W\Gamma \tag{10}$$

and in the wake, the circulation in the corresponding annulus is :

$$B\Gamma = 2\pi rFwt \tag{11}$$

let the circulation Γ in Eq. (10) equal to that in Eq. (11) will ultimately determine that circulation distribution Γ (r) that minimizes the induced power of the propeller .

In order to obtain Γ (r), it is necessary to relate wt to a more measurable quantity. The motion of the fluid must be normal to the local vortex sheet, and this normal velocity is w_n. Therefore, the tangential velocity is given by :

$$W_t = w_n sin\phi \tag{12}$$

the axial velocity of the vortex filament would be :

$$v' = w_n / cos\phi \tag{13}$$

where the increase in magnitude of v' over w_n is due to rotation of the filament. This is analogous to a barber pole where it appears that the stripes are translating in spite of the fact that only a rotational velocity exists. It will become clear that it is convenient to use v', and the corresponding displacement velocity ratio, $\zeta = v'V$. The tangential velocity is then given by :

$$W_t = V\zeta sin\phi cos\phi \tag{14}$$

the circulation can be expressed as :

$$\Gamma = \frac{2\pi r V^2 \zeta G}{B\omega} \tag{15}$$

$$G = F sin\phi cos\phi \tag{16}$$

To impose the Condition for minimum energy Loss [16], a departure from Larrabee's design procedure is considered. The momentum equations and the circulating equations, are required to be equivalent. This condition results in the interference factors being related to ζ by the equations :

$$a = \left(\zeta/2\right) \cos^2 \phi \left(1 - \epsilon \tan \phi\right) \tag{17}$$

$$a' = \left(\zeta/2x\right) \cos \phi \sin \phi \left(1 + \epsilon/ \tan \phi\right) \tag{18}$$

where Eqs. (15) and (16) have been used to expressL' in terms of ζ, and the terms in epsilon correctly describe the viscous contribution. Equations (17,18), together with the geometry of the above figure (6) lead to the important simple relation :

$$\tan \phi = \left(1 + \zeta/2\right) x = \left(1 + \zeta/2\right) \lambda/\xi \tag{19}$$

Here, λ is a constant, and ξ varies from ξ_o at the hub to unity at the edge of the disc. The relation between the two nondimensional distances and the constant speed ratio is :

$$X = \omega r/v = \left(r/R\right)/\lambda = \xi/\lambda \tag{20}$$

Recalling the Betz condition, r tan ϕ = const, Eq. (19) proves that for the vortex sheet to be a regular screw surface, ζ must be a constant independent of radius. This is the condition for minimum energy loss.

To derive the Constraint Equations for design procedures, it is necessary to specify either T, delivered by the propeller or the power P, delivered to the propeller. The nondimensional thrust and power coefficients used for design are :

$$T_c = 2T/\left(\rho V^2 \pi R^2\right) \tag{21}$$

$$P_c = 2P/\left(\rho V^3 \pi R^2\right) = 2Q\Omega/\left(\rho V^3 \pi R^2\right) \tag{22}$$

And using these definitions, Eq. (5,6) can be written as

$$T_c' = I_1' \zeta - I_2' \zeta^2 \tag{23}$$

$$p_c' = J_1'\zeta + J_2'\zeta^2 \tag{24}$$

where the primes denote derivatives with respect to ξ, and

$$I_1' = 4\xi G\left(1 - \epsilon\tan\phi\right) \tag{25}$$

$$I_2' = \lambda\left(I_1'/2\xi\right)\left(1 + \epsilon/\tan\phi\right)\sin\phi\cos\phi \tag{26}$$

$$J_1' = 4\xi G\left(1 + \epsilon/\tan\phi\right) \tag{27}$$

$$J_2' = \left(J_1'/2\right)\left(1 - \epsilon\tan\phi\right)\cos^2\phi \tag{28}$$

Note : Superscript ($'$) = derivative with respect to ξ . Noted Since e is constant for an optimum design, if power is specified, the constraint relations are :

$$\zeta = -\left(J_1/2J_2\right) + \left(\left(J_1/2J_2\right)^2 + P_c/J_2\right)^{1/2} \tag{29}$$

$$T_c = I_1\zeta - I_2\zeta^2 \tag{30}$$

where the integration has been carried out over the region $\xi = \xi_o$ and $\xi = 1$

III. Design Procedures

Based on Adkins and Liebeck's work [15], the design is initiated with the specified conditions of power (or thrust), hub and tip radius, rotational rate, free stream velocity, number of blades, and a finite number of stations at which blade geometry is to be determined. Also, the design lift coefficient per station if it is not constant must be specified. and then we can get all dimensions and angles of the blade.

The design then proceeds in the following steps :

1) Select an initial estimate for ζ ($\zeta = 0$ will work).

2) Determine the values for F and ϕ at each blade station by Eqs(31)and (34).

$$F = \frac{2}{\pi}\arccos e^{-f} \tag{31}$$

$$f = \frac{\frac{B}{2}\left(1 - \xi\right)}{\sin\phi_t} \tag{32}$$

$$\tan\phi_t = \left(1 + \zeta/2\right)\lambda \tag{33}$$

$$\tan\phi = \frac{\left(\tan\phi_t\right)}{xi} \tag{34}$$

3) Determine the product Wc, and Reynolds number For the element dr of a single blade at radial station r, let C_l the local lift coefficient. Then, the lift per unit radius of one blade is

$$\rho W^2 c C_L/2 = \rho W \Gamma \tag{35}$$

Where Γ is given by eq.(15) . it follows directly that :

$$W_c = \frac{4\pi\lambda G V R\zeta}{C_L B} \tag{36}$$

and Reynolds number would be :

$$Re = \frac{Wc}{\nu} \tag{37}$$

Assume for the moment that ζ is known; then the local value of ϕ is known from equation (34), and the above relation is a function only of the local lift coefficient. Since the local Reynolds number is W_c divided by the kinematic viscosity, equation (37) plus a choice for C_l will determine the Reynolds number and , from the airfoil section data. The total velocity is then determined by :

$$W = \frac{V\left(1+a\right)}{sin\phi} \tag{38}$$

Where (a) is given by Eq. (17), and the chord is then known from Eq. (36,38). If the choice for C_l causes ϵ to be a minimum.

4) Determine ϵ and a from airfoil section data.

5) Determine$a$ and a' from Eq. (17,18), and W from Eq. (38).

6) Compute the chord from step (3), and the blade twist $\beta = \alpha+\phi$.

7) Determine the four derivatives I and J from Eq. (25,28) and numerically integrate these from $\xi = \xi_o$ to $\xi = 1$.

8) Determine ζ and Tc from Eqs. (29) and (30).

9) If this new value for ζ is not sufficiently close to the old one (e.g., within 0.1%) start over at step 2 using the new ζ.

10) Determine propeller efficiency.

The analysis method is outlined here in order to discuss problems of convergence at off design.A correction for the placement of the factor F used by Glauert in his equation, this requires the interference factors to be as follow :

$$a = \frac{\sigma K}{\left(F - \sigma k\right)} \tag{39}$$

$$a' = \frac{\sigma k'}{\left(F + \sigma K'\right)} \tag{40}$$

$$k = \frac{C_y}{\left(4 \sin^2 \phi\right)} \tag{41}$$

$$k' = \frac{C_x}{\left(4 \cos \phi \sin \phi\right)} \tag{42}$$

$$\tan \phi = \frac{V \left(1 + a\right)}{\Omega r \left(1 - a'\right)} \tag{43}$$

The analysis procedure requires an iterative solution for the flow angle ϕ at each radial position, ξ An initial estimate for ϕ can be obtained from Eq. (19) by setting ζ equal to zero. Since β is known, the value for α equal β-ϕ, and the airfoil coefficients are known from the section data. The Reynolds number is determined from the known chord and W, which is obtained from Eq. (39), and the new estimate for ϕ is then found from Eq. (43). A direct substitution of the new ϕ for the old value will cause adequate convergence for an optimum design which is being analyzed at the design point. However, for analysis off-design and for non optimum designs, some recursive combination of the old and new values for ϕ is required to cause adequate convergence. Under some conditions (usually near the tip), convergence may not be possible at all due to large values for the interference factors, a and a', in Eq. (39,40). Since F is zero at the tip and a is not for a square tip propeller, the value for a is - 1 and a' is +1. Such values are physically impossible since the slipstream factors are approximately twice the values at the rotor plane. For resolving this problem, clipping the magnitude of a(N) and$a'N$ at the value of a(N-1) and a'(N-1). For analysis, the conventional thrust and power coefficients are :

$$C_T = \frac{T}{\rho n^2 D^4} \tag{44}$$

$$C_p = \frac{P}{\rho n^3 D^5} \tag{45}$$

Using Eqs. (3) and (5), the differential forms with respect to (f) are given by :

$$C_T' = \frac{\frac{\pi^3}{4} \sigma C_y \xi F^{32}}{\left(\left(F + \sigma K'\right) \cos \phi\right)^2} \tag{46}$$

When these have been integrated from the hub to the tip, the propeller efficiency is :

$$\eta = \frac{C_T J}{C_P} \tag{47}$$

IV. Implemented software using Matlab with graphical user interface "GUI"

A software design tool is developed using MATLAB software to design such propeller scale. A graphical user interface (GUI) is also added for more simplicity for enhancing various designs. Figure 7 shows a block diagram for the design hierarchy With inputs such as rpm, power, diameter, airfoil shape, airplane velocity and number of blades. A

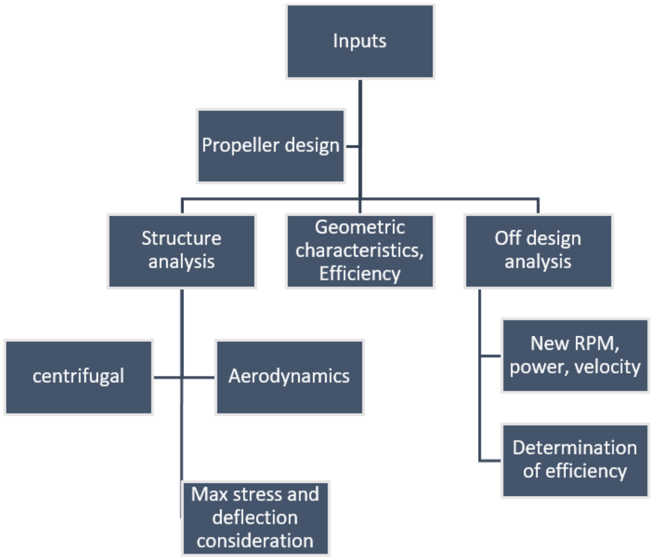

FIGURE 7 Hierarchical class structure to represent MTC Propeller software

complete design of the propeller is achieved and a 3D model is obtained with conjunction with the numerical results results in a parametric design software. Figures from figure 8 to figure 10 present a snap shots for the designed GUI.

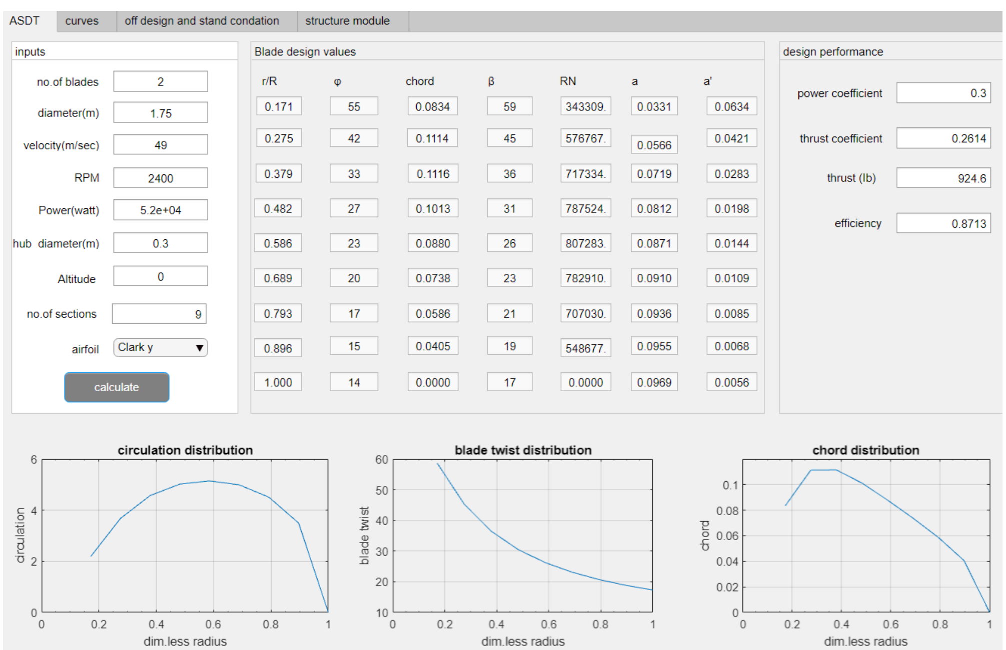

FIGURE 8 Graphical user interface (1) of the implemented software

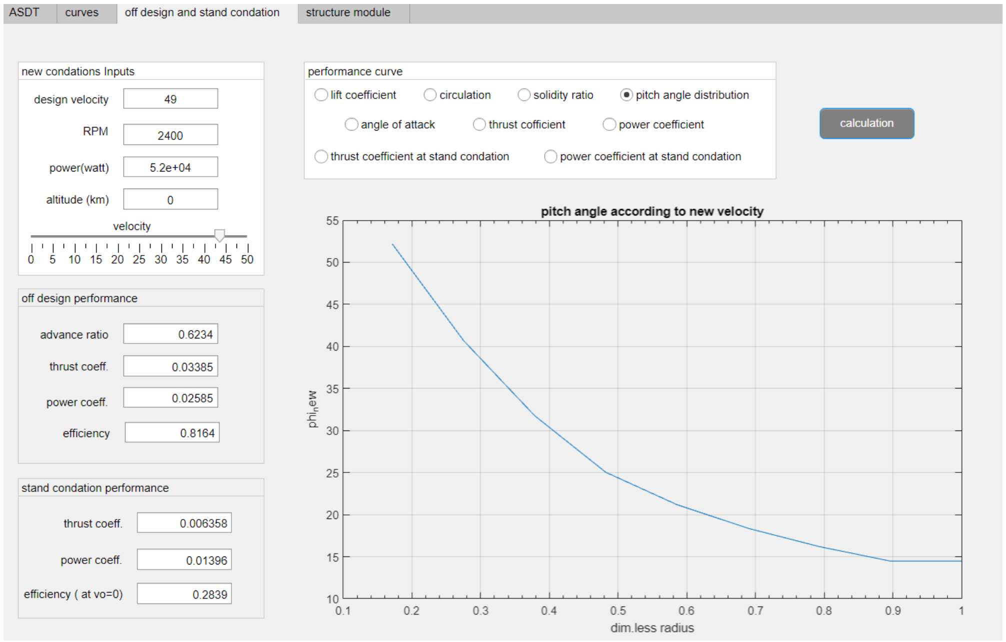

Figure 9 **Graphical user interface (2) of the implemented software**

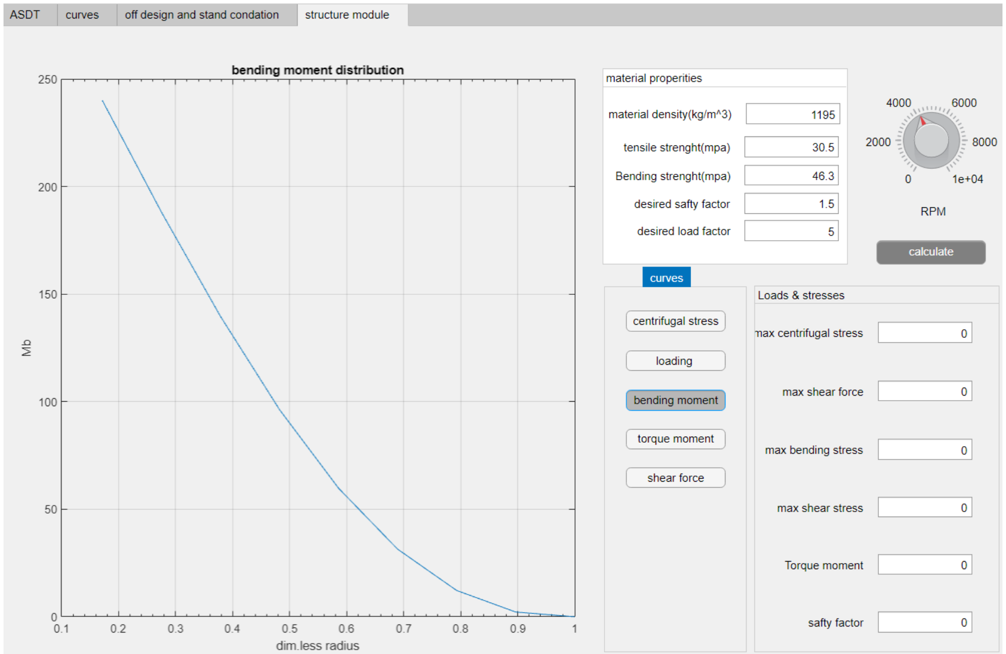

Figure 10 **Graphical user interface (3) of the implemented software**

V. case study and software validation

The output results from the implemented software have been checked and compared with the results of Adkins and Liebeck[15]. The required input data for Adkins and Liebeck case study are described in Table 1 :

Figures **??** show the results obtained for the case study introduced by Adkins and Liebeck and the implemented software. The results show a very good matching with by having the same input data introduced by Ref.[15].

Table 1 Required data for propeller design

Input data for propeller design		Units
Power	52000	kW
Rotation Speed	2400	RPM
Hub Diameter	0.3	m
Tip Diameter	1.75	m
Aircraft Velocity	49	m/s
Lift Coefficient	0.7	-
No. of Blades	2	-

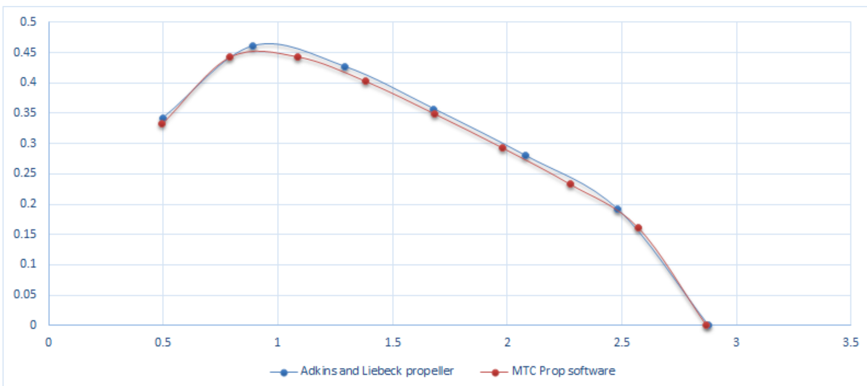

Figure 11 Comparison between chord length distribution along span towards blade tip

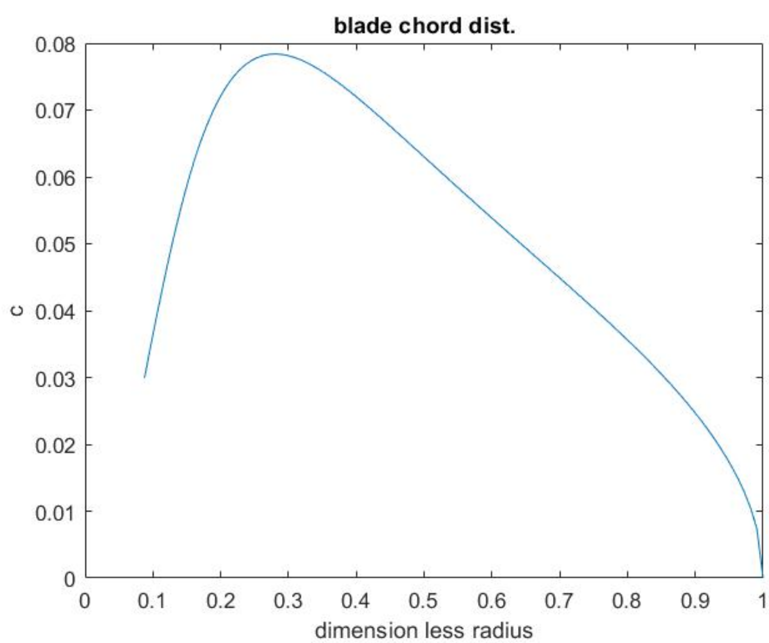

Figure 12 Chord length distribution along blade span in (m)

Figure 15 shows a 3D CAD model based on the obtained dimensions from the software. A technological link

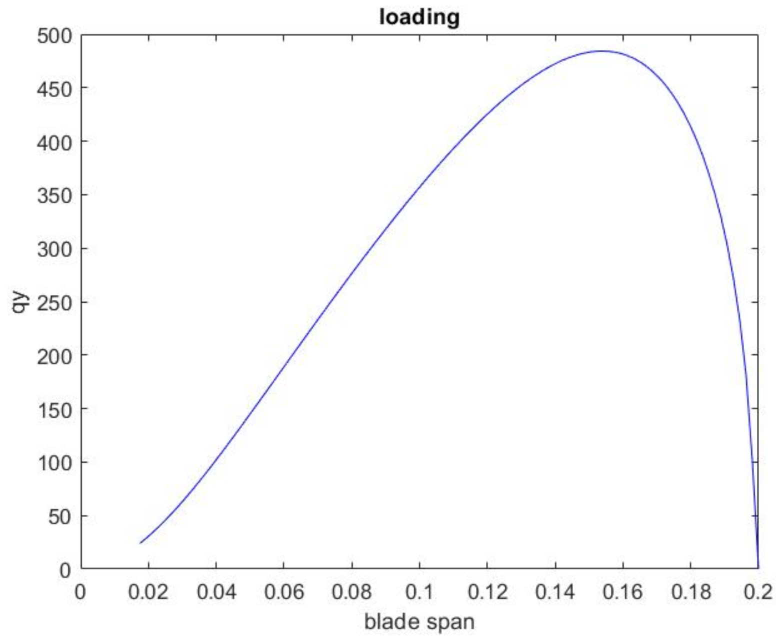

Figure 13 Aerodynamic lift force per unit length (N/m)

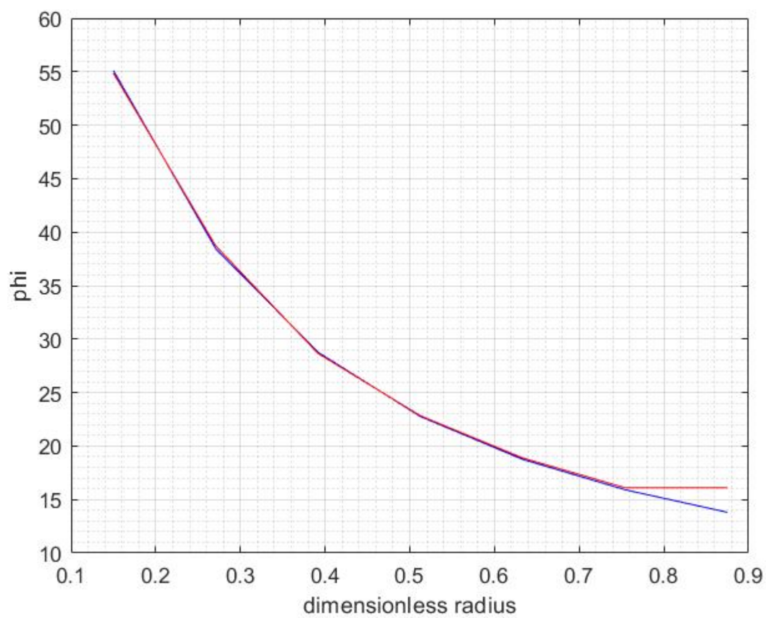

Figure 14 Off design matching with design at the same conditions (phi in deg)

between the Matlab software and the CAD modeling software in order to parametrize the input conditions in order to enhance the design process.

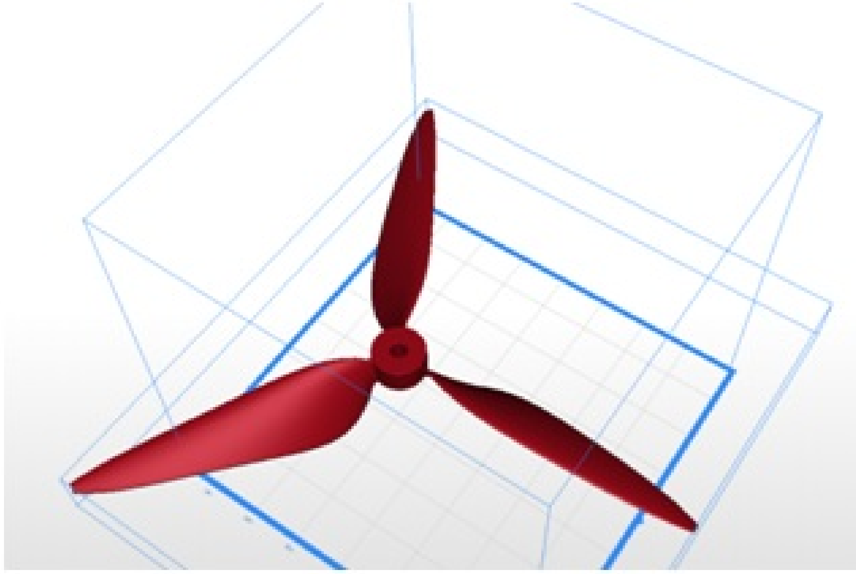

Figure 15 Printed blade cad 3D view

VI. Conclusion

In this work, a complete design procedures as well as a graphical user interface were obtained for small scale propellers. The aerodynamic model is started using a mission required input for a specific small flying vehicle to obtain the required thrust. The designed GUI is able to define each technological design step including operating, structural and goemetrical characterestics of the proposed propeller. A case study of an already existing propeller was used to verify the design modeling procedures. The efficiency of the propulsion system does not depend solely on the propeller, but it is affected significantly by the motor efficiency and the vehicle characteristics[17]. Thus, as a future work, it is important to include the motor characteristics in the design process.

Références

[1] Ash, R., Miley, S., Landman, D., and Hyde, K., "Propeller performance of Wright brothers"Bent End'propellers," *36th AIAA/ASME/SAE/ASEE Joint Propulsion Conference and Exhibit*, 2000, p. 3152.

[2] Betz, A., "with appendix by Prandtl," *L.," Screw propellers with Minimum Energy Loss," Göttingen Reports*, 1919, pp. 193–213.

[3] Glauert, H., "Airplane propellers," *Aerodynamic theory*, Springer, 1935, pp. 169–360.

[4] Theodorsen, T., "The Theory of Propellers IV : Thrust, Energy, and Efficiency Formulas for Single-and Dual-rotating Propellers with Ideal Circulation Distribution," 1944.

[5] Larrabee, E. E., "Practical design of minimum induced loss propellers," Tech. rep., SAE Technical Paper, 1979.

[6] Adkins, C., and LIEBECK, R., "Design of optimum propellers," *21st Aerospace Sciences Meeting*, 1983, p. 190.

[7] Dayhoum, A., Zakaria, M. Y., Elshabka, A. M., and Abdelhamid, O. E., "Speculation of local aerodynamic loads on helicopter rotor blade in forward flight," *IOP Conference Series : Materials Science and Engineering*, Vol. 610, 2019, p. 012099. doi :10.1088/1757-899x/610/1/012099, URL `https://doi.org/10.1088%2F1757-899x%2F610%2F1%2F012099`.

[8] Zakaria, M. Y., Nemnem, A. F., Dayhoum, A., Elnady, T., and Elzahaby, A., "Centimeter Scale Micro Wind Turbine Modelling Correction Using Wind Tunnel Experiments," *AIAA Scitech 2019 Forum*, 2019, p. 1577.

[9] Zakaria, M. Y., Nemnem, A. F., Gad, K., and Abdelwahab, M. M., "Performance Analysis and Aerodynamic Modeling of Contra-Rotating Ducted fan UAV," *AIAA Scitech 2019 Forum*, 2019, p. 1788.

[10] Law, A., "OATmedia launches PPL training book set," 2008.

[11] Thiele, M., Obster, M., and Hornung, M., "Aerodynamic Modeling of Coaxial Counter-Rotating UAV Propellers," *VFS, 8th Biennial Autonomous VTOL Technical Meeting*, 2019, p. 13.

[12] Ghoddoussi, A., "A more comprehensive database for propeller performance validations at low Reynolds numbers," Ph.D. thesis, Wichita State University, 2016.

[13] Mccormick, J. T., "Propeller blade," , Nov. 16 1948. US Patent 2,453,803.

[14] Prandtl, L., "Appendix to" Schraubenpropeller mit geringstem Energieverlust'by Betz, A," *Gottinger Nachr*, 1919, pp. 193–217.

[15] Adkins, C. N., and Liebeck, R. H., "Design of optimum propellers," *Journal of Propulsion and Power*, Vol. 10, No. 5, 1994, pp. 676–682.

[16] Larrabee, E. E., and French, S. E., "Minimum induced loss windmills and propellers," *Journal of Wind Engineering and Industrial Aerodynamics*, Vol. 15, No. 1-3, 1983, pp. 317–327.

[17] Garner, W., "Model Airplane Propellers," *Air-Propeller research document, wbgarner08@ verizon. net*, 2009.